Articles

Fluorescence Imaging of Reactive Oxygen Metabolites Generated in Single Macrophage Cells (NR8383) upon Phagocytosis of Natural Zeolite (Erionite) Fibers

John F. Long,[1] Prabir K. Dutta,[2] and Brian D. Hogg[2]

[1]Department of Veterinary Biosciences; and [2]Department of Chemistry, The Ohio State University, Columbus, Ohio 43210 USA

In this paper we address the phenomenon of reactive oxygen metabolite generation subsequent to phagocytosis of mineral fibers by macrophages. Natural erionite fibers were chosen because of their established toxicity. Macrophages (cell line NR8383) were loaded with the dye 5-(and 6)-carboxy-2′,7′-dichlorodihydrofluorescein diacetate and exposed to erionite particles by centrifuging cells and fibers together to effect adherence. Reactive oxygen metabolite generation was examined by monitoring the fluorescence of oxidized dye formed via the reaction with oxygen species produced during phagocytosis. Individual cells were repeatedly scanned for up to 2 hr to monitor the evolution of this fluorescence. It was found that erionite-exposed cells had a mean total fluorescence of three times that of controls during the first 35 min, declining to two times that of controls at 35–60 min and about the same level as that of controls at 60–80 min. Ultrastructural studies of similarly treated aliquots of cells showed marked variation in size and numbers of the phagocytized particles. This study demonstrates that intracellular oxidation can be monitored on a single cell basis over a period of time. Quantitative studies are in progress to establish the relationship between the phagocytized particulate load and the extent of fluorescence. *Key words*: 5-(and 6)-carboxy-2′,7′-dichlorodihydrofluorescein diacetate, erionite, fluorescence imaging, macrophage, mineral fiber, peroxide. *Environ Health Perspect* 105:706–711 (1997)

With the extensive use of naturally occurring and synthetic mineral fibers, there is need for a method of assaying the fibers for potentially harmful biologic activity. While it is acknowledged that animal testing must be used as a component of the testing procedure, preliminary *in vitro* procedures may serve to identify fibers with high potential for harmful biologic activity. An objective of this paper is to supply certain basic information toward the development of such an *in vitro* technique. *In vitro* methods also are of value in elucidating the mechanisms of fiber toxicity.

It is now generally accepted that both form and chemical reactivity need to be considered in assessing the overall toxicity of a fibrous material (*1*). In the past, most research concentrated on the effects of fiber morphology, and the importance of fiber form and dimension is now fully acknowledged. The limited investigations in the area of chemical reactivity have generally dealt with surface chemistry studies on isometric dusts, such as silica (*1–3*) or carbons (*1*). Surface modification of amosite asbestos by hydrocarbon chains altered its pathogenic properties (*4*), further suggesting a role for surface chemistry in the biologic response to minerals.

One of the responses associated with phagocytosis of fibrous minerals by macrophages is the increased generation of reactive oxygen metabolites (ROMs). The association of ROMs with asbestos-related toxicity has been supported by studies of a number of research groups in recent years (*5,6*). Furthermore, the addition of antioxidants markedly reduces the pathogenetic effect of asbestos fibers (*7*). Also, the addition of iron chelators (*5,8*) minimized ROM release, indicating the importance of the surface composition of the fiber.

There are several methods reported to measure the oxidative burst during phagocytosis. In studies based on the chemiluminescent response of luminol (*9,10*) as a measure of ROM, the data suggest that there is no difference in ROM production between pathogenic and nonpathogenic dusts. However, in this method, the measured effect arises from interaction of the particle with the outer surface of the cytoplasmic membrane. Assays to measure superoxide ion generation by cytochrome c reduction also measure extracellular oxygen species and have elicited different responses from different fibers, in contrast to those reported in the luminol study (*11*).

We wish to develop methodologies in which the molecular message—which is transmitted from the fiber surface to the cell—can be more precisely examined. To do this, it is necessary to determine if the ROM generated within a cell upon phagocytosis varies depending on the surface of the fiber. This requires intracellular measurements, ideally, on a single cell basis. Information on a single cell basis can be obtained by flow cytometric methods, but such methods are limited in that the ROM level is recorded at only one point in time, thus precluding repeated measurements on the same cell. Likewise, the intracellular localization of the ROM generation cannot be recorded because the measurement is limited to a single whole-cell measurement.

We have recently reported a laser fluorescence imaging technique that makes possible the examination of the development of ROM in single macrophage (NR8383) cells upon phagocytosis of naturally occurring

Address correspondence to J.F. Long, Department of Veterinary Biosciences, The Ohio State University, 1925 Coffey Road, Columbus, Ohio 43210 USA.
We acknowledge the support of the Office of Research, The Ohio State University, for support of this research. We are also grateful to R.J. Helmke for providing the macrophage line. We thank L. Mathes for helpful discussions.
Received 3 January 1997; accepted 7 April 1997.

erionite fibers (*12*). This technique has been employed by previous researchers for quantitative fluorescence measurements including, among others, the measurement of exogenous peroxide within cells (*13*) and the measurement of intracellular glutathione levels (*14*). Moreover, measurement of ROM within neurons (*15*) and determinations of cellular DNA using propidium iodide (*16*) were also performed using a variation of the technique described here.

Although several chemical dyes have been suggested as markers of oxidative metabolism, perhaps the most thoroughly studied is the dye 2′,7′-dichlorodihydrofluorescein diacetate (H_2DCF-DA) (*17–19*). The reduced ester is essentially nonpolar and crosses the cell membrane. Once inside, the esters are hydrolyzed by (nonspecific) cellular esterases. The resulting diol is more polar and thus better retained by the cell membrane. For our experiments, this ester cleavage is reasonable because Helmke and co-workers (*20,21*) reported that the NR8383 cell line (the cell line used in our study) exhibits high nonspecific esterase activity. The diol is oxidized by ROM to the fluorescent form (DCF) and is detected by excitation at a wavelength of 488 nm [oxidation of the diol occurs readily, but reaction with superoxide is dubious (*19*)]. Work with H_2DCF-DA showed significant loss in intracellular levels after 1 hr, a finding similar to that reported by Royall and Ischiropoulos (*22*). Thus, the carboxylated form, 5-(and 6)-carboxy-2′,7′-dichlorodihydrofluorescein diacetate (C-H_2DCF-DA) was used for these studies. The carboxyl substituent makes the marker more polar. As a result of the increased polarity, the C-H_2DCF-DA is retained longer, as compared to H_2DCF-DA, but requires increased concentrations and longer incubations during loading.

In this paper, we extend our study of macrophage (NR8383)-erionite fiber interaction using laser fluorescence imaging. Our focus continues to be on natural erionite fibers because of their well-demonstrated toxicity (*12*). We investigate the evolution of ROM generation in individual cells at timed intervals following cell–particle contact and show significant cell-to-cell variability. We used electron microscopy to examine the ultrastructural cellular features after interaction with erionite and also to provide information about the variability of cellular response.

Materials and Methods

Cells. The cells used were from a rat lung alveolar macrophage cell line (NR8383). The culture was obtained through the cooperation of R.M. Helmke, University of Texas (San Antonio, TX). The cells have been extensively characterized, and their ability to generate an oxidative burst has been shown (*20,21*). Since the evaluation of the oxidative burst is the endpoint in this study, this cell line was chosen because it possessed this feature. Aliquots of cells frozen from the original stock were thawed periodically and used to assist in maintaining target cell uniformity.

Culture methods. The cells were cultured at 37°C in 5% CO_2 using Hams F12 medium with 15% fetal bovine serum (Sigma Chemical, St. Louis, MO) and were maintained in 30-ml polystyrene culture flasks (Costar, Cambridge, MA). For use in the subsequent experimental procedures, aliquots of cells were grown in 15-ml polypropylene centrifuge tubes (Life Science Products, Denver, CO) to minimize cell adherence. For use of the erionite fibers in tissue culture, the samples were subjected to 125°C for 6 hr for sterilization.

Dye. 5-(and 6)-carboxy-2′,7′-dichlorodihydrofluorescein diacetate (C-H_2DCFH-DA) was purchased from Molecular Probes, Eugene, Oregon.

Test particles. The naturally occurring erionite mineral sample (#27091, Pine Valley, Nevada) used in this study was obtained from Minerals Research (Clarkson, NY). The high content of erionite in the sample was demonstrated by X-ray diffractometry as reported previously (*12*). The erionite sample, being of natural origin, had the expected variability in size and shape ranging from colloidal size to fibers 10–15 μm in length. To obtain a narrower size distribution, the following steps were developed. Initially, the sample was equilibrated in a balanced salt solution. It was then swirled, vortexed 5 min, sonicated, and allowed to settle 5 min. The volume was 10 ml and the diameter of the glass container was 2 cm. The aliquot removed for study was collected from the upper one-third of the suspension in order to exclude the larger particles (which would be too large for effective phagocytosis). Aliquots of the cell-fiber mixtures were examined by light microscopy to assure appropriate proportions.

The Zymosan A sample (heat killed yeast particles) was obtained from Sigma Chemical Company, St. Louis, Missouri.

Establishment of cell-fiber contact of dye-loaded cells. The study was designed so that multiple cells were exposed to multiple particles. Cells (~200,000/ml) were washed by centrifugation, supernatant was removed, and cells were resuspended in ACAS buffer [formulation described by Hogg et al. (*12*)]. The cells were allowed to equilibrate with buffer during 30 min incubation at 37°C in 5% CO_2. Equilibrated cells were then exposed to C-H_2DCF-DA (final concentration, 60 μM) and incubated at 37°C in 5% CO_2 for 40 min. The cells were then removed from incubation and immediately chilled in an ice-water bath at 4°C to induce metabolic inactivity. ACAS buffer (1 ml; control) or fiber suspension (1 ml) in buffer (~1.4×10^6 particles/ml by hemocytometer count) was then added to the chilled cells; cells were then vortexed briefly and centrifuged (~600 rpm for 5 min) at this same (4°C) temperature to promote contact of the fibers with the cell surface. The supernatant containing debris and excess dye was removed and discarded. The pelleted cells (including cells with adherent fibers) were immediately resuspended in chilled ACAS buffer. This cell–fiber mixture was then taken to the fluorescence spectrometer, transferred to a warmed Lab-Tek chambered coverglass (NUNC, Inc., Naperville, IL), and rapidly warmed to 37%C in a temperature-controlled chamber on the microscope.

ACAS 570 interactive laser cytometer. For the detection and quantitation of ROM, we used an ACAS 570 Interactive Laser Cytometer (Meridian Instruments, Okemos, MI). The ACAS 570 used an accousto-optically modulated Ar-ion laser tuned to 488 nm to excite the fluorescence in the cells. Emission at wavelengths >515 nm was filtered and detected with a photomultiplier tube. The microscope optics used for focusing the laser were coupled to a video camera, which allowed for real-time visualization of the sample volume. The confocal microscope enabled fluorescence imaging to be collected from thin (0.8 μm) sections of the cell in as rapidly as 1 min per slice, depending on the size of the image. The advantages of confocal microscopy in studying phagocytic systems has been previously discussed in the literature (*23*). Sample chambers were clipped to the piezoelectrically driven stage; 0.1 μm-step coordinates of stage positions were recorded by the ACAS 570 and allowed the user to easily return to a specific slide position (such as a previously viewed cell).

Procedure for electron microscopy. The cells (aliquots) were fixed in 3% glutaraldehyde. Following overnight fixation, the cells were rinsed with cacodylate (0.1 M) using two 15-min rinses and placed in osmium tetraoxide for 1 hr. Cells were then dehydrated (using alcohols progressively from 50% to 100%) for 30 min each. They were then embedded in Medcast (Ted Pella, Inc., Redding, CA). The cells were then examined using a Philips 300 microscope (Phillips Electronics Inst. Co., Mahwah, NJ) to evaluate their ultrastructural morphology.

Technique for cytochrome c assay. Extracellularly released ROMs may be

detected by reaction with exogenous ferricytochrome c (*24*). Briefly, 2.0 ml cell suspension (about 1.5 million cells by hemocytometer count) was added to polypropylene test tubes and kept on ice. Next, 1.0 ml of test agent (12 million particles of erionite by hemocytometer count or 1 ml buffer for controls) was added to the ice-cold suspension. Cytochrome c stock solution (61 µl) was then added (final concentration of cytochrome = 40 µM), and the entire suspension was then vortexed and placed in a bath at 37°C for 60 min. After incubation, the suspensions were placed on ice, and cells and particles were removed by centrifugation. The resulting supernatant was examined for ferrocytochrome c content using a Shimadzu (Columbia, MD) UV-265 UV-visible spectrometer with 3 ml buffer in the reference cell. An extinction coefficient of 24.8 l/mmol/cm at 549 nm was obtained by measuring the absorbance of 40 µM ferrocytochrome c (obtained by reduction with excess sodium dithionite and with continuous N_2 gas bubbling) and was employed for quantitation. Spectra were digitized and were then analyzed using Galactic Industries' Grams/386 for Microsoft Windows (Version 1.06A; Microsoft, Redmond, WA).

Control tests to evaluate viability of cells treated with dye/fibers. Two methods were undertaken to test whether any component of cell processing was sufficient to affect viability during the period of the runs.

Propidium iodide (PI; Molecular Probes, Eugene, OR) was added to 2 ml erionite-exposed cell suspension in buffer to a final concentration of 15 µg PI/ml, and cells were immediately analyzed for PI fluorescence using the ACAS 570. Cell membranes were made permeable by the addition of Tween-20 (one hanging droplet) to 2 ml of cell solution.

For ultrastructural evaluation, aliquots of cells were given timed exposures to the erionite preparation to correlate with time intervals used for the fluorescence procedures for ROM measurement. Thus, intervals of 20, 40, and 60 min (plus an extra time interval of 24 hr) were used. At the end of these time intervals, the cells (aliquots) were fixed in 3% glutaraldehyde. They were then processed as described in Materials and Methods and examined to evaluate their ultrastructural integrity.

Mean cellular fluorescence at timed intervals subsequent to the cell–fiber contact. To study the temporal relationship of total cell fluorescence (ROM generation) following the cell–fiber contact (using the time the cell–fiber preparations were warmed from 4°C to 37°C to restore cell metabolic activity), cells were pre-loaded with C-H_2DCF-DA [see Hogg et al. (12)]. The software-generated position coordinates for representative cells were noted, and fluorescence scans were then repeated periodically on the same cells to eliminate the variability that would be inevitable if different cells were used in the timed studies.

Results

Oxidative burst following erionite/macrophage contact using the cytochrome c assay. Table 1 demonstrates extracellular oxidative metabolism. The data represent the reduction of cytochrome c after a 1-hr incubation period. The control group received no particulates (1 ml buffer), whereas the other spectra are from 12 million particles (suspended in a 1-ml aliquot). Both the zymosan- and the erionite-stimulated cells forced an increase in absorption at the 549-nm peak for ferrocytochrome c equivalent to 3.2 nmol reduced cytochrome. The use of zymosan established the oxidative burst ability of the cells.

Particle size distribution and phagocytosis. The adherence of the test particles to the target cell upon centrifugation was examined by light microscopy (Fig. 1). The process of engulfment could be observed usually within a few minutes at 37°C. With this natural fiber source, there was a marked range in particle lengths, with sizes from colloidal to about 10–15 µm in length.

Intracellular localization of fluorescence associated with C-H_2DCF-DA oxidation indicating ROM generation. As reported in our original description of the technique (*12*), the fluorescence from the oxidized dye indicates the intracellular generation of ROM. Figure 2 illustrates DCF fluorescence from one erionite-exposed cell (Fig. 2A, B) and one control cell (Fig. 2C, D). Each pic-

Table 1. Cytochrome c assay

	Absorbance at 549 nm	Absorbance control	Cytochrome c released (µM)
Control (buffer)	0.001_8	–	0.07
Erionite exposed	0.027_9	0.026_1	1.05
Zymosan exposed	0.028_6	0.026_8	1.08

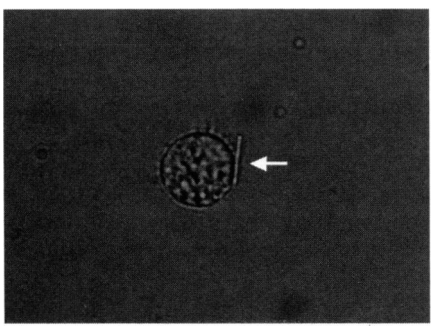

Figure 1. An individual macrophage (NR8383) with erionite fiber (arrow) adhered.

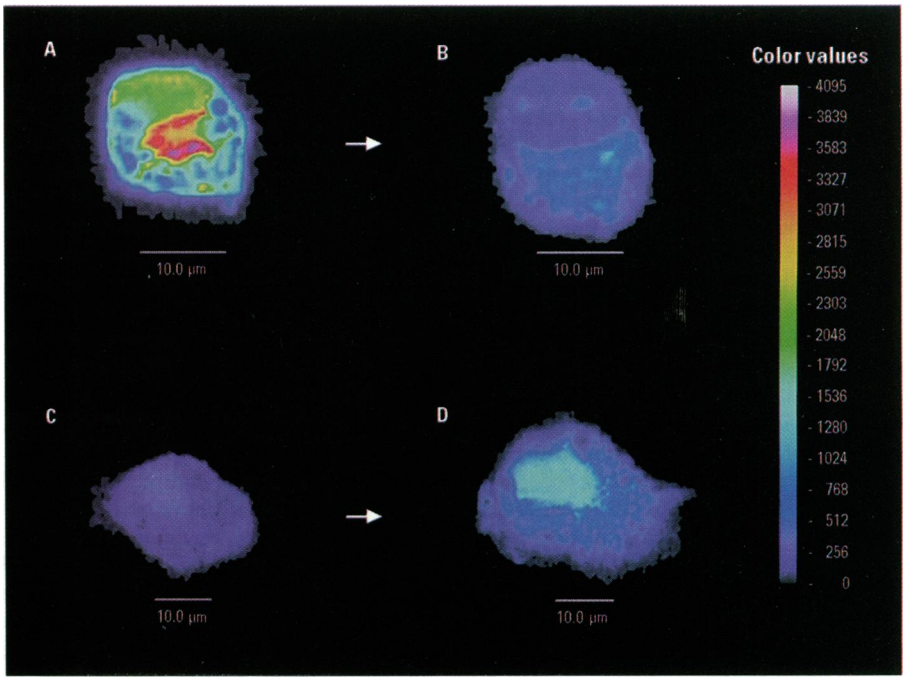

Figure 2. (A) Fluorescence in a macrophage 24 min postexposure to erionite (showing the maximum fluorescence). (B) The same cell at 56 min postexposure (at a time when the fluorescence typically is fading). Typical fluorescence in a control macrophage at (C) 22 min and (D) at 57 min after warming (in controls, the low initial fluorescence gradually increases with time). The color scale indicates fluorescence intensity.

tured cell represents one confocally focused region of approximately 0.8 µm thickness. The erionite-exposed cell was imaged at 24 and 56 min (Fig 2A and Fig. 2B, respectively) after removal from the ice bath and warming. The representative control cell (no erionite exposure) shows fluorescence levels established at 22 and 57 min (Fig. 2C and Fig 2D, respectively). Clearly, the fiber-exposed cell illustrates stronger fluorescence at the 20–25 min mark when compared to the control.

Sharply delineated fluorescence characteristically evolves within fiber-exposed cells during the period up to 90 min following the cell–fiber contact. Typically, the nucleus remains free of fluorescence. This fluorescence-free area (determined by imaging) correlates well with the location of the cell nucleus, as shown in real time on the simultaneously projected optical-microscope image associated with the ACAS. There are often multiple smaller foci of fluorescence within the cell; it is not possible to identify these foci from the image, but their size and distribution are compatible with structures such as mitochondria or peroxisomes. In addition, there are generally spherical foci of fluorescence. These are often intensely fluorescent (indicating ROM generation) and in sharp contrast to less fluorescent adjacent areas of the cell. These cannot be identified from the simultaneously projected image, and whether these may represent phagosomal areas could not be determined.

Cellular fluorescence of erionite-exposed cells compared to control cells. Regardless of the identity of organelles associated with fluorescence, from the initial inspection of scans it appears that there is an overall elevation of cellular fluorescence in the erionite-exposed cells compared to controls. This is evident from Figure 3 in which three summed confocal slices of cellular fluorescence for each cell (both the erionite-exposed and control cells) are plotted in relation to time.

The first 10 min was required for the cells and particles to settle and become adhered to the glass floor of the chambered coverglass and to have their coordinates determined. During this time, the temperature in the chamber was raised from 4°C to 37°C, thus restoring the normal metabolic activity. Once started (at 10–20 min), the scans and imaging continued intermittently until approximately 90 min had elapsed.

Inspection of the graph shows marked variability of the fiber-exposed cells and lesser variability of the control cells. It also shows the erionite-exposed cells to be higher in fluorescence than controls during much of the period, especially in the early stages. For the 20–40 min period, the erionite-exposed cells had a mean cellular fluorescence more than three times that of controls. During the 40–60 min period, the erionite-exposed cells had a mean cellular fluorescence still more than twice that of controls. Only during the 60–80 min period did the mean erionite cellular fluorescence decline to a level relatively indistinguishable compared to controls.

Maintenance of cell viability following ingestion of erionite fibers. PI is widely accepted as a DNA/RNA marker. Upon intercalation within DNA, fluorescence intensity increases and the emission maximum shifts from 639 to 615 nm (*25*). However, healthy cell membranes remain impervious to PI, and it may therefore be used as a marker for the weakened membranes characteristic of moribund cells. Recent viability assays using propidium iodide have marked dead sperm cells (*26*) and human natural killer cells (*27*).

In our studies, Tween-20 was used to make cells permeable to PI. The addition of the detergent caused increased nuclear fluorescence within 5 min. Such fluorescence served as a benchmark for comparison of dead and living cells. Erionite-exposed cells, prepared with PI as described above, showed no increase in PI fluorescence during the 80 min tested. The few erionite-exposed cells that showed any increase were dead at the start of fluorescence imaging and would have been excluded from ROM studies based on poor morphology. Dead or apparently dying cells were excluded from assays based on crenated, blebbed, or otherwise atypical membrane appearance.

Erionite fibers and particles were routinely observed to be within cells by optical microscopy, indicating completeness of phagocytosis. To examine the particle intake at higher resolution, samples were examined by electron microscopy at 20, 40, 60, and 90 min after fiber–cell contact.

After a 20 min period following the contact of the fiber with metabolically active cells (and warming the chamber to 37°C to restore metabolic activity), the fibers were characteristically found to be intracellular and within lysosomes (Fig. 4, 5). Sometimes the volume of the erionite-containing lysosome (Fig. 6) increased in size, due to what appeared to be fluid (based on its electron lucent, homogeneous, fine ultrastructure, and in having a space-occupying location around the fibers). The lysosomal membrane ranged from appearing to be completely intact morpho-

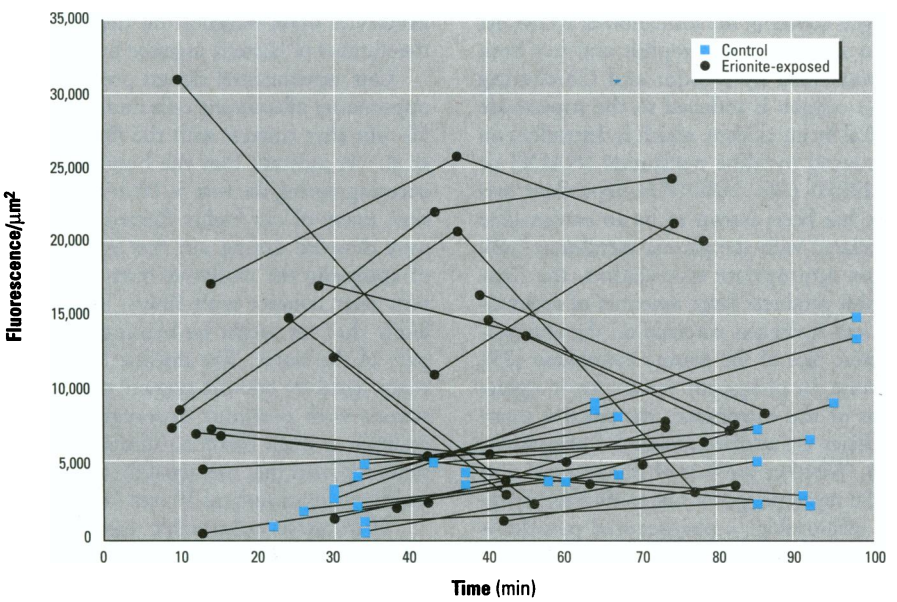

Figure 3. Fluorescence intensity of erionite-exposed cells versus control cells over 100 min. Each line connects data points for an individual cell over time.

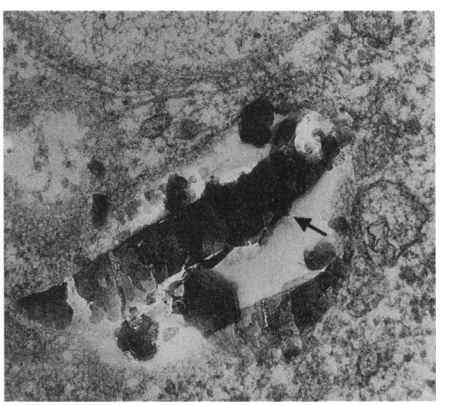

Figure 4. Mineral fiber (arrow) plus fragments in a lysosome. The fiber morphologically resembles those seen by scanning electron microscopy in samples of erionite (×18,000) (*12*).

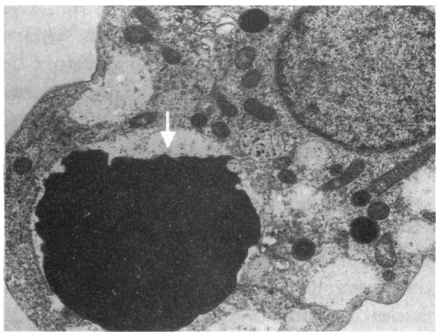

Figure 5. Mineral particle (arrow) within a lysosome with a morphologically intact membrane (×8,700).

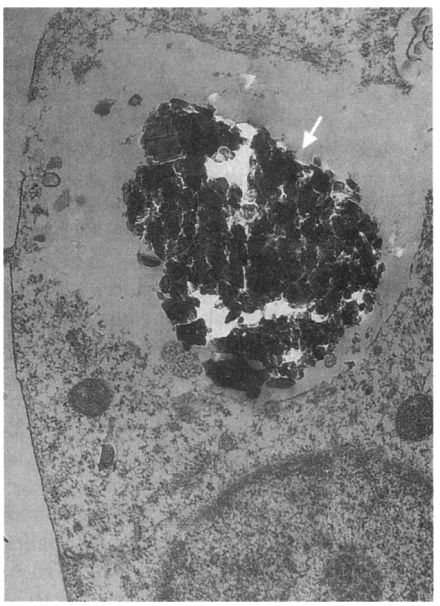

Figure 6. Mineral particle (arrow) within a lysosome. The volume of the lysosome appears to have increased, the particle appears fragmented, and the membrane appears not to be intact (×15,100).

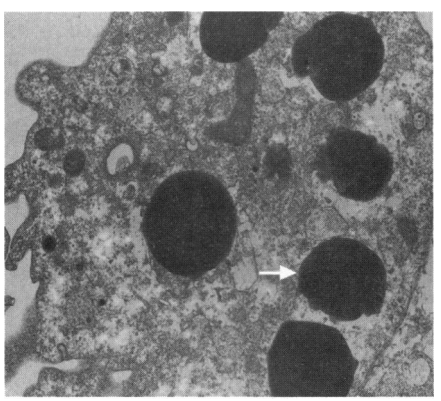

Figure 7. Macrophage with multiple particles, which are apparently within lysosomes. ×12,100. The arrow points to a particle apparently within a lysosome.

logically (Fig. 5) to having obvious interruption in its continuity (Fig. 6). Frequently, multiple colloidal-size particles were seen within individual lysosomes (Fig. 7), which sometimes nearly coalesced. Aside from these lysosomal-associated changes, no specific morphologic change was noted in any other membranes or organelles during the time frame (90 min) used in the study.

Discussion

Cell line NR8383, with its well-characterized ability to generate an oxidative burst (*20,21*), was useful in this study. We observed evidence of an oxidative burst subsequent to the exposure of NR8383 macrophages to erionite fibers. This was detected by a cytochrome c assay on a cell population basis, as well as in individual cells, as shown by fluorescence with the ACAS interactive laser cytometer. This was compatible with the findings of Hansen and Mossman (*11*), who also used cytochrome c with macrophages exposed to erionite.

Experiments with PI and the ultrastructural studies indicate that the cells remain viable after prolonged contact with the erionite preparation as well as the handling procedures in the assay. The cells remained impervious to PI after 80 min. Thus, the observed oxidation of the dye arises from the oxidative burst and/or metabolic processes and not from cell death and associated activity.

The circumscribed foci of the fluorescence cannot at this time be distinctly related to specific organelle changes, as seen by ultrastructurally evaluated aliquots of macrophages with ingested erionite particles and viewed at corresponding time intervals. The mechanism by which the reduction of oxygen occurs in the formation of ROM has been studied in neutrophils and has been summarized by Bender and Chickering (*28*); oxygen is reduced to the superoxide radical by an oxidase, which is dependent on a reduced pyridine nucleotide (NADH or NADPH) (*28*). NAD(P)H-dependent oxidase has been shown to be an ectoenzyme associated with the plasma membrane (*28*). Upon appropriate stimulation, the neutrophil produces large amounts of superoxide and hydrogen peroxide on the anticytoplasmic face of the plasma membrane (*29*). Because the phagocytic vesicles are invaginations of this membrane, the reactive intermediates are released inside the phagosome (*30*). Whether the foci of fluorescence seen in the macrophages in our study have a similar relationship to phagocytized particles is not known at this time.

Likewise, it is not known whether structural interruptions of lysosomal membranes (Fig. 6) enable the extension of ROM generation to occur beyond the margins of the phagosomes or whether the membranes may have increased permeability (even though ultrastructurally intact in appearance). Allison et al. (*31*) studied the uptake of silica by lung macrophages. The particles of silica were initially found within phagosomes. The uptake of silica apparently rendered the membrane of the lysosomes unstable, and hydrolytic enzymes were ultimately released into the cell with injury resulting. The silica particles were also released during the process; the particles were then reengulfed, which led to necrosis. The process leading to necrosis is thought to be due to a chemical reaction between the silica and components of the lysosomal membrane. It is possible that a similar phenomenon may be associated with the phagocytized erionite particles.

The rise in mean cellular fluorescence of erionite-exposed cells was evident as an early event. Within 35 min after exposure to erionite, the mean cellular fluorescence was more than three times that of controls. The reason for the higher variability of fluorescence in erionite-exposed cells may be related to variation in size and number of erionite particles in the cells. Some cells show five or six particles within lysosomes, while others have as few as one or even none. In previous studies on dust-induced macrophage chemiluminescence, Vilím et al. (*9*) noted that the luminol signal depended on the ratio of fibers to cells. Using latex beads, Kobzik et al. (*32*) observed a rise in fluorescence in cells, roughly in proportion to numbers of phagocytized beads, as assayed by dichlorofluorescin using flow cytometry. A similar effect was observed by Szejda et al. (*18*), who found that the amount of oxidative products formed by polymorphonuclear leukocytes upon phagocytosis depended on the number of bacteria ingested by the cells.

Our experimental design precludes the opportunity of scanning cells during the first 10 min after contact with the fibers. Vilím et al. (*9*) indicate that the burst could be occuring during the first 5–10 min. In addition, many of our higher fluorescent values were detected during our first opportunity of observing the oxidative burst at 10–15 min after contact with fibers. Thus, it is likely that we might be missing the early part of the burst. The decline in fluorescence signal for erionite-exposed cells is consistent with previous observations. For example, a study based on luminol fluorescence reported that the signal decreased after reaching a maximum at 10 min (*10*).

There are several possible reasons for the gradual decline in fluorescence in this study. The cessation of the oxidative burst should leave behind a steady state concentration of oxidized dye. However, it has been noted by Royall and Ischiropolous (*22*) that increased

membrane permeability allows oxidized dye to diffuse out from the cell. Another possibility is intracellular acidification, which quenches the dye fluorescence (*15*). The creation of a highly acid environment within the vacuole is thought to play a supporting role in the microbicidal activity of the phagocyte (*33*). The pH would however have to drop below 5 to significantly influence the DCF fluorescence (*18*).

The reason for the gradual rise in fluorescence of the controls could be from mitochondria-induced generation of ROM. Reynolds and Hastings (*15*) also noted an increase in fluorescence in control neuron cells and proposed that it could be due to laser-light activated oxidation of the dye.

The evidence presented here suggests that the increased fluorescence indicates where in the cell ROM generation is occurring. This method, therefore, provides the opportunity for intracellular study of the pathophysiologic changes associated with cellular exposure to mineral fibers.

To further refine the study, it will be necessary to bring about uniformity of the fiber–cell exposure. Here we have single cells interacting with fibers of variable size and numbers. Experiments are being designed in which a single fiber is given to a single cell, thus providing an opportunity for both quantitation and localization of ROM generation. The technique to demonstrate the intracellular generation of reactive oxygen metabolites could be used with other relevant cell types (such as cells obtained by lung lavages) to further the understanding of the pathogenesis of mineral fiber toxicity.

References

1. Fubini B. The possible role of surface chemistry in the toxicity of inhaled fibers. In: Fiber Toxicology (Warheit DB, ed). New York: Academic Press, 1993;229–257.
2. Wiessner JH, Henderson JD Jr, Sohnle PG, Mandel NS, Mandel GS. The effect of crystal structure on mouse lung inflammation and fibrosis. Am Rev Respir Dis 138:445–450 (1988).
3. Vallyathan V, Castranova V, Pack D, Leonard S, Shumaker J, Hubbs AF, Shoemaker DA, Ramsey DM, Pretty JR, McLaurin JL. Freshly fractured quartz inhalation leads to enhanced lung injury and inflammation. Am J Respir Crit Care Med 152:1003–1009 (1995).
4. Brown RC, Carthew P, Hoskins JA, Sara E, Simpson CF. Surface modification can affect the carcinogenicity of asbestos. Carcinogenesis 11:1883–1885 (1990).
5. Goodglick LA, Kane AB. Role of reactive oxygen metabolites in crocidolite asbestos toxicity to mouse macrophages. Cancer Res 46:5558–5566 (1986).
6. Rom WN, Travis WD, Brody AR. Cellular and molecular basis of the asbestos-related diseases. Am Rev Respir Dis 143:408–422 (1991).
7. Mossman BT, Marsh JP, Shatos MA. Alteration of superoxide dismutase activity in tracheal epithelial cells by asbestos and inhibition of cytotoxicity by antioxidants. Lab Invest 54:204–212 (1986).
8. Kennedy TP, Dodson R, Rao NV, Ky H, Hopkins C, Baser M, Tolley E, Hoidal JR. Dusts causing pneumoconiosis generate ·OH and produce hemolysis by acting as Fenton catalysts. Arch Biochem Biophys 269:359–364 (1989).
9. Vilím V, Wilhelm J, Brzák P, Hurych J. Stimulation of alveolar macrophages by mineral dusts *in vitro*: luminol-dependent chemiluminescence study. Environ Res 42:246–256 (1987).
10. Gormley IP, Kowolik MJ, Cullen RT. The chemiluminescent response of human phagocytic cells to mineral dusts. Br J Exp Pathol 66: 409–416 (1985).
11. Hansen K, Mossman BT. Generation of superoxide from alveolar macrophages exposed to asbestiform and nonfibrous particles. Cancer Res 47:1681–1686 (1987).
12. Hogg BD, Dutta PK, Long JF. *In vitro* interaction of zeolite fibers with individual cells (macrophages NR8383): measurement of intracellular oxidative burst. Anal Chem 68: 2309–2312 (1996).
13. Aucoin MM, Barhoumi R, Kochevar DT, Granger HJ, Burghardt RC. Oxidative injury of coronary venular endothelial cells depletes intracellular glutathione and induces HSP 70 mRNA. Am J Physiol 268:H1651–H1658 (1995).
14. Burghardt RC, Barhoumi R, Lewis EH, Bailey RH, Pyle KA, Clement BA, Phillips TD. Patulin-induced toxicity: a vital fluorescence study. Toxicol Appl Pharmacol 112:235–244 (1992).
15. Reynolds IJ, Hastings TG. Glutamate induces the production of reactive oxygen species in cultured forebrain neurons following NMDA receptor activation. J Neurosci 15:3318–3327 (1995).
16. Srivastava V, Miller S, Busbee D. Immunofluorescent evaluation of DNA repair synthesis using interactive laser cytometry. Cytometry 14:144–153 (1993).
17. Bass DA, Parce JW, DeChatelet LR, Szejda P, Seeds MC, Thomas M. Flow cytometric studies of oxidative product formation by neutrophils: a graded response to membrane stimulation. J Immunol 130:1910–1917 (1983).
18. Szejda P, Parce JW, Seeds MS, Bass DA. Flow cytometric quantitation of oxidative product formation by polymorphonuclear leukocytes during phagocytosis. J Immunol 133:3303–3307 (1984).
19. LeBel CP, Ischiropoulos H, Bondy SC. Evaluation of the probe 2′,7′-dichlorofluorescin as an indicator of reactive oxygen species formation and oxidative stress. Chem Res Toxicol 5:227–231 (1992).
20. Helmke RJ, Boyd RL, German VF, Mangos JA. From growth factor dependence to growth factor responsiveness: the genesis of an alveolar macrophage cell line. In Vitro Cell Dev Biol 23:567–574 (1987).
21. Helmke RJ, German VF, Mangos JA. A continuous alveolar macrophage cell line: comparisons with freshly derived alveolar macrophages. In Vitro Cell Dev Biol 25:44–48 (1989).
22. Royall JA, Ischiropoulos H. Evaluation of 2′,7′-dichlorofluorescin and dihydrorhodamine 123 as fluorescent probes for intracellular H_2O_2 in cultured endothelial cells. Arch Biochem Biophys 302:348–355 (1993).
23. Hook GR, Odeyale CO. Confocal scanning fluorescence microscopy: a new method for phagocytosis research. J Leukocyte Biol 45:277–282 (1989).
24. Cohen HJ, Chovaniec ME. Superoxide generation by digitonin-stimulated guinea pig granulocytes. J Clin Invest 61:1081–1087 (1978).
25. Arndt-Jovin DJ, Jovin TM. Fluorescence labeling and microscopy of DNA. In: Methods in Cell Biology, vol 30 (Taylor DL, Wang Y-L, eds). New York:Academic Press, 1989;417–448.
26. Garner DL, Johnson LA. Viability assessment of mammalian sperm using SYBR-14 and propidium iodide. Biol Reprod 53:276–284 (1995).
27. Shenker BJ, Vitale LA, Keiba I, Harrison G, Berthold P, Golub E, Lally, ET. Flow cytometric analysis of the cytotoxic effects of *Actinobacillus actinomycetemcomitans* leukotoxin on human natural killer cells. J Leukocyte Biol 55:153–160 (1994).
28. Bender HS, Chickering WR. Superoxide, superoxide dismutase and the respiratory burst. Vet Clin Pathol 12:7–14 (1983).
29. Gabig TG, Babior BM. The O_2-forming oxidase responsible for the respiratory burst in human neutrophils. J Biol Chem 254:9070–9074 (1979).
30. Halliwell B, Gutteridge JMC, Cross CE. Free radicals, antioxidants, and human disease: where are we now? J Lab Clin Med 119:598–620 (1992).
31. Allison AC, Harington JS, Birbeck M. An examination of the cytotoxic effects on silica on macrophages. J Exp Med 124:141–154 (1966).
32. Kobzik L, Godleski JJ, Brain JD. Oxidative metabolism in the alveolar macrophage: Analysis by flow cytometry. J Leukocyte Biol 47:295–303 (1990).
33. Ryan TC, Weil GJ, Newburger PE, Haugland R, Simons ER. Measurement of superoxide release in the phagovacuoles of immune complex-stimulated human neutrophils. J Immunol Methods 130:223–233 (1990).